



Open Archive Toulouse Archive Ouverte (OATAO)

OATAO is an open access repository that collects the work of Toulouse researchers and makes it freely available over the web where possible.

This is an author-deposited version published in: <http://oatao.univ-toulouse.fr/>
Eprints ID: 11494

Identification number: DOI : 10.1016/j.quaint.2006.12.021

Official URL: <http://dx.doi.org/10.1016/j.quaint.2006.12.021>

To cite this version:

De Vleeschouwer, François and Van Vliët-Lanoé, Brigitte and Fagel, Nathalie and Richter, Thomas and Boës, Xavier *Development and application of high-resolution petrography on resin-impregnated Holocene peat columns to detect and analyse tephrae, cryptotephrae, and other materials*. (2008) *Quaternary International*, vol. 178 (n° 1). pp. 54-67. ISSN 1040-6182

Any correspondence concerning this service should be sent to the repository administrator:
staff-oatao@inp-toulouse.fr

Development and application of high-resolution petrography on resin-impregnated Holocene peat columns to detect and analyse tephtras, cryptotephtras, and other materials

François De Vleeschouwer^{a,*}, Brigitte van Vliët-Lanoé^b, Nathalie Fagel^a,
Thomas Richter^c, Xavier Boës^a

^a*Unité de Recherche Argiles et Paléoclimats, Université de Liège, Allée du 6 Août, B18, Sart Tilman, B 4000 Liège, Belgium*

^b*UMR 8110 CNRS Processus et Bilans des Domaines Sédimentaires, Université Sciences et des Technologies de Lille, SN5,
B 59655 Villeneuve d'Ascq cédex, France*

^c*Department of Marine Chemistry and Geology, Royal Netherlands Institute for Sea Research (NIOZ), P.O. Box 59, 1790 AB Den Burg (Texel Island),
The Netherlands*

Abstract

We describe the potential for high-resolution detection, observation and chemical analysis of tephtras and cryptotephtras in freeze-dried and resin-impregnated peat sections. Special attention is drawn to tephtra grain alteration products, sensitive to standard lab treatment, but preserved using an impregnation technique developed here. Resulting blocks and thin sections provide a continuous archive of tephtras that can be investigated through a wide range of non-destructive techniques encompassing polarising and fluorescence microscopy, scanning electron microscopy with/without elemental analysis, and XRF-based core scanning.

1. Introduction

Tephtra studies have proved their usefulness in a broad range of fields including Quaternary chrono-stratigraphy, paleoenvironmental studies, soil sciences, eruption hazards, paleoclimate and archaeology (e.g. Naranjo and Stern, 1998; Newnham et al., 1998; Sadler and Grattan, 1999; Wulf et al., 2004). Various techniques are used to detect and characterise tephtra such as microscopic observations (polarising, fluorescence, scanning electron microscopy), geochemistry (e.g. Larsen et al., 1999), grain-size (e.g. Fisher, 1964), and dating (e.g. Okuno et al., 2003). However, the interpretation of these analyses, and particularly those leading to a correlation framework over large distances, can be biased by the lack of recognition of diminutive distal cryptotephtras. Discrete mm- to cm-scale (i.e. proximal) tephtra layers are easily recognised in sedimentary sequences, while thinner (i.e. distal) tephtras

could be strongly weathered (e.g. Hodder et al., 1991), bioturbated, or simply invisible to the naked eye, and easily missed. This is particularly the case in peat bog records when scattered tephtra grains may be dark-stained and difficult to distinguish from the dark brown organic matrix. In this context, several studies have demonstrated the importance of high-resolution observations and detailed description of distal tephtras with the aim of obtaining a high-quality tephrostratigraphic framework (e.g. van den Bogaard and Schmincke, 2002; Gehrels et al., 2006). Tracing cryptotephtras (e.g. Gehrels et al., this volume) provides new insights into the world of cryptotephtra, but is often limited by sampling resolution (often 1 cm at best). Non-destructive techniques such as X-radiography (e.g. Dugmore and Newton, 1992) and fresh core scanning (e.g. Caseldine et al., 1999) have been used to detect tephtra and cryptotephtra in fresh cores. However, in situ observations are often needed prior to manual collection, to characterize better the succession of tephtras recorded in a peat sequence, especially if several thin tephtras are deposited in a small thickness of peat. Moreover, alteration products

*Corresponding author. Tel.: +32 4 366 22 10; fax: +32 4 366 22 02.
E-mail address: fdeveleschouwer@ulg.ac.be (F. De Vleeschouwer).

often coating grains may be washed out or modified during lab treatment prior to microscopic observation or single-grain analyses.

Impregnation techniques have been used successfully in lake sediments (e.g. Lotter and Lemcke, 1999; Boës and Fagel, 2005), and can be applied to peat cores to provide a continuous record of tephras in sediment through thin sections. This technique has the advantage of archiving the tephra preserved in the sample. In this paper, we present: (1) a new method of impregnation of peat cores containing macroscopic and microscopic tephras; (2) a range of observations on impregnated blocks and thin sections using various techniques, with emphasis on the alteration of tephra grains; and (3) a range of geochemical techniques that can be applied to analysing tephras preserved in impregnated peat blocks. These main goals are approached using impregnated peat D-cores from southeast Belgium and peat box cores from northeast Iceland (Vopnafjordur area, 65°44' N–15°54' W).

2. Methodology

2.1. Collecting, handling, and sampling peat

Peat collection can be achieved in two main ways: coring or box cutting. Coring is generally completed by using a Belo-Russian-type stainless steel D-corer (e.g. Jowsey, 1965), which removes a semi-cylindrical core 25–50 cm long and 3–10 cm diameter. Cores are wrapped in plastic film and bagged into PVC tubes. The ideal sample size for subsequent impregnation and analysis is a D-core section of 10-cm long and at least 4 cm in diameter. Two cores must be collected, as near as possible to each other in order to minimise lateral variation. One core is dedicated to impregnation while the other is reserved for manual tephra collection or further analyses.

In the case of peat outcrops, monoliths can be carved using a cutting tool, wrapped in plastic film, bagged in PVC boxes and finally cut from the section with a nylon cutting cord. Although a 10-cm long, 5-cm wide and 2-cm thick “block” is sufficient, larger monoliths are easier to cut in the field. Blocks dedicated to impregnation can then be sub-sampled. We cut 20 × 10 × 7 cm boxes out of the outcrop and sub-sampled 10-cm-long, 1-cm-thick slices from the side of each block (Fig. 1). After 1 × 2 cm-samples are removed for pollen analysis, the remaining slices are dedicated to impregnation. The remaining box sample is cut in 1-cm-thick samples dedicated to further analyses such as dating, geochemistry and macrofossil studies. If selective manual tephra collection is planned, the remaining block should not be cut.

To avoid drying of the peat, critical for impregnation (see Section 2.2), all samples need to be stored in a cooled room or fridge. Boës and Fagel (2005) emphasised minimising post-coring disturbance, which is essential to preserve the thinnest mineral layers. Therefore if sub-sampling for impregnation is needed, as in box cutting, it should be achieved as a first step by cutting a large enough block. Any other sub-sampling should be completed after retrieving the block to be impregnated.

2.2. Freeze-drying and impregnation

Methods of impregnation by resin polymer are well developed for unconsolidated sediments such as soils (e.g. Tippkötter and Ritz, 1996) and lacustrine sediments (e.g. Boës and Fagel, 2005). A review of the different techniques developed for polymer impregnation along with full references is given by Boës and Fagel (2005). The basic steps are: (1) water removal (i.e. dehydration), (2) resin impregnation and (3) drying, sawing and thin-section preparation. Common methods of dehydration encompass either full water substitution by acetone in liquid (e.g.

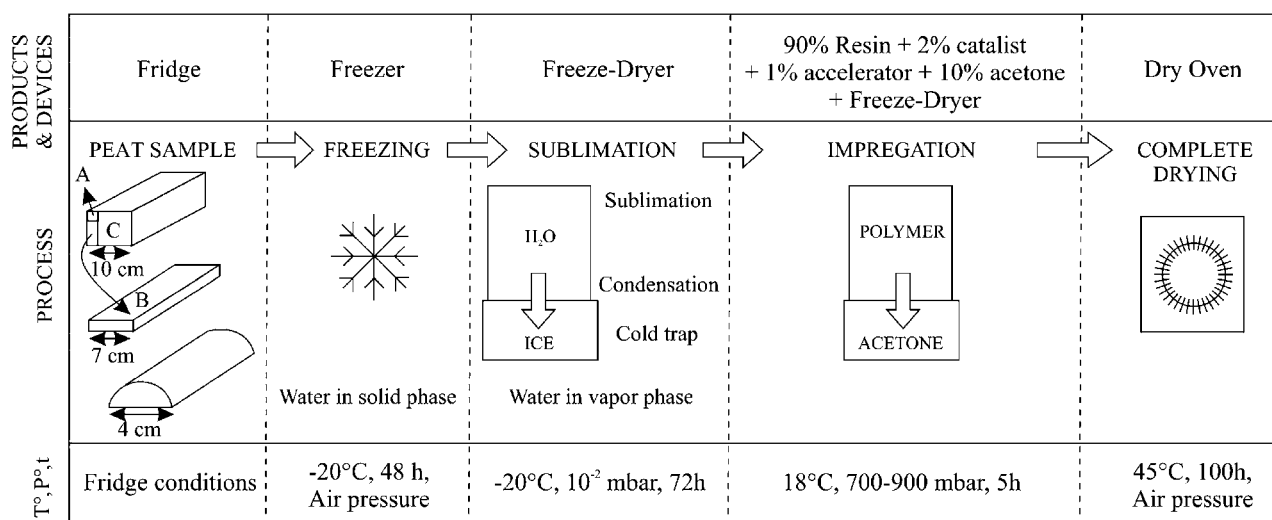


Fig. 1. Schematic sketch of sub-sampling and impregnation technique. For more details on impregnation, see Boës and Fagel (2005). (A) Samples for pollen analyses. (B) Sample for impregnation. (C) Samples for other analyses.

Pusch, 1999) or vapour phase (Camuti and McGuire, 1999), or water evaporation by oven-drying or freeze-drying (e.g. Francus, 1998). Impregnation is commonly achieved by acetone–resin-exchange under vacuum (e.g. Boës and Fagel, 2005). Various polymers have been used to accomplish impregnation (e.g. Tippkötter and Ritz, 1996). Among these products, epoxy polymers are the most widely used (e.g. Francus, 1998).

Because of their high water and organic content, peat cores are especially difficult to impregnate (*see below*), and few laboratories have assigned a specific technique for such organic-rich sediments (e.g. Mackenzie and Dawson, 1961; Takeda, 1988). Water removal by simple evaporation or oven drying is not recommended for peat samples because of their high water content (up to 95 wt-%) resulting in shrinkage when desiccated, eliminating any possibility to reconstruct a 1:1 scale log. Full water substitution by acetone should also be avoided because acetone causes physical stress within the peat by dissolving organic matter and weakening plant cells, thus modifying potentially the sediment to some degree. The preferred method for impregnating peat is freeze-drying followed by impregnation under vacuum. The technique presented in this paper is adapted from that described by Boës and Fagel (2005) for lacustrine sediment.

Preparation of peat samples requires a deep-freezing (freezer, 12 h. at -20°C) and freeze-drying using a LIOVAC GT3 freeze-dryer in order to sublimate ice (e.g. Pike and Kemp, 1996) (Fig. 1). Peat saturation by resin is performed under low vacuum (700–900 mbar depending on peat density) with a polymer resin (Norsodyne S 2010 V, Cray Valley) mixed with 0.2% of catalyst (Interox), 0.1% of accelerator (Octoate Cobalt 49) and less than 10% acetone, progressively added to the dried samples (for more details, see Boës and Fagel, 2005). A maximum of 10% acetone should be used to prevent organic matter decomposition. Following polymerisation, samples are slowly dried at 45°C .

Thin sections up to 68 mm by 140 mm are mounted by gluing a glass slide on the polished impregnated block using pure resin (i.e. same resin mix but without acetone). Freshly glued slides need to be constrained under a load for 24 h. After complete drying, the impregnated samples are sawed and slides are polished using diamond discs until about 50–100 μm thick. They are finally covered using a standard cover glass and the same resin mix (without acetone).

2.3. Possible problems encountered during impregnation

The main problems encountered during impregnation relate to sample size. Larger samples are more challenging and require a longer freeze-drying and impregnation process. If freeze-drying is not complete for large samples, remaining ice needles could melt and hydrate the plastic, leading to hardening problems. This problem can be resolved with a longer freeze-drying time. An additional

problem is the relatively high viscosity of the polymer. Because the requirement to minimise dilution using acetone (<10%) the resin may not entirely impregnate the sample to its centre, even under high vacuum. This problem is the most delicate to solve, because an increase of the vacuum or of the acetone content of the polymer mix could disturb the sediment matrix. Pressure and acetone content must be optimised according to peat texture and composition. When composed of *Sphagnum* mosses, the peat is highly porous and easy to impregnate. Conversely, when composed of *Carex* or *Molinia*, peat could be more compact, in a poorer state of conservation, or both. The resin mix should be thinned by adding 5% more acetone. Peat samples with abundant mineral grains or with common intercalated tephra layers are typically impregnated with a normal resin mix (less than 10% acetone).

An additional problem may occur when dealing with organic-rich sediment containing fine mineral layers such as tephra. During the freeze-drying process, the higher pore space (and higher water content) of the tephra relative to the peat may induce shrinkage and crack propagation in the tephra layer. This tephra will still be in place, but with a small 1–2 mm crack (see e.g. C1, Section 3.2, Fig. 4A).

3. Applications in petrography

3.1. Optical microscopy

Direct observation by an optical microscope provides information about botanical components of the peat. The type of vegetation can be identified, such as *Sphagnum* peat, *Carex* peat, *Eriophorum* peat, wood fragments or roots. However, taxonomic determinations are not as accurate as in classical plant macrofossil studies (e.g. see ACCROTELM Project website at <http://www2.glos.ac.uk/accrotelm>) because thin sections provide only two-dimensional observations. At best, observations can be carried out to family, or genus level. However, the arrangement of macrofossils together with their state of preservation can be observed. For example, Figs. 3A–E are optical microscope images from a *Sphagnum*-dominated peat bog from the Hautes Fagnes Plateau, southeast Belgium (see Fig. 2). Fig. 3A (30 cm depth) displays well-preserved *Sphagnum* stems and leaves. Fig. 3B (45 cm depth) displays compacted *Sphagnum* tissues, followed by a progressive degradation of organic matter (Fig. 3C and 1D, respectively 50 and 80 cm depth) around the largest plant macrofossils and a shift in peat composition. Other undefined mosses are present together with *Sphagnum*. Further down core (Fig. 3E, 640 cm down core), organic matter is highly decomposed, and plant macrofossils are poorly preserved and thus indeterminate.

A second organic feature that can be observed in impregnated thin sections is the occurrence of macro- and micro-charcoal layers. The systematic counting of charcoal can provide insight into fire history and indications on past ecological conditions and human impact

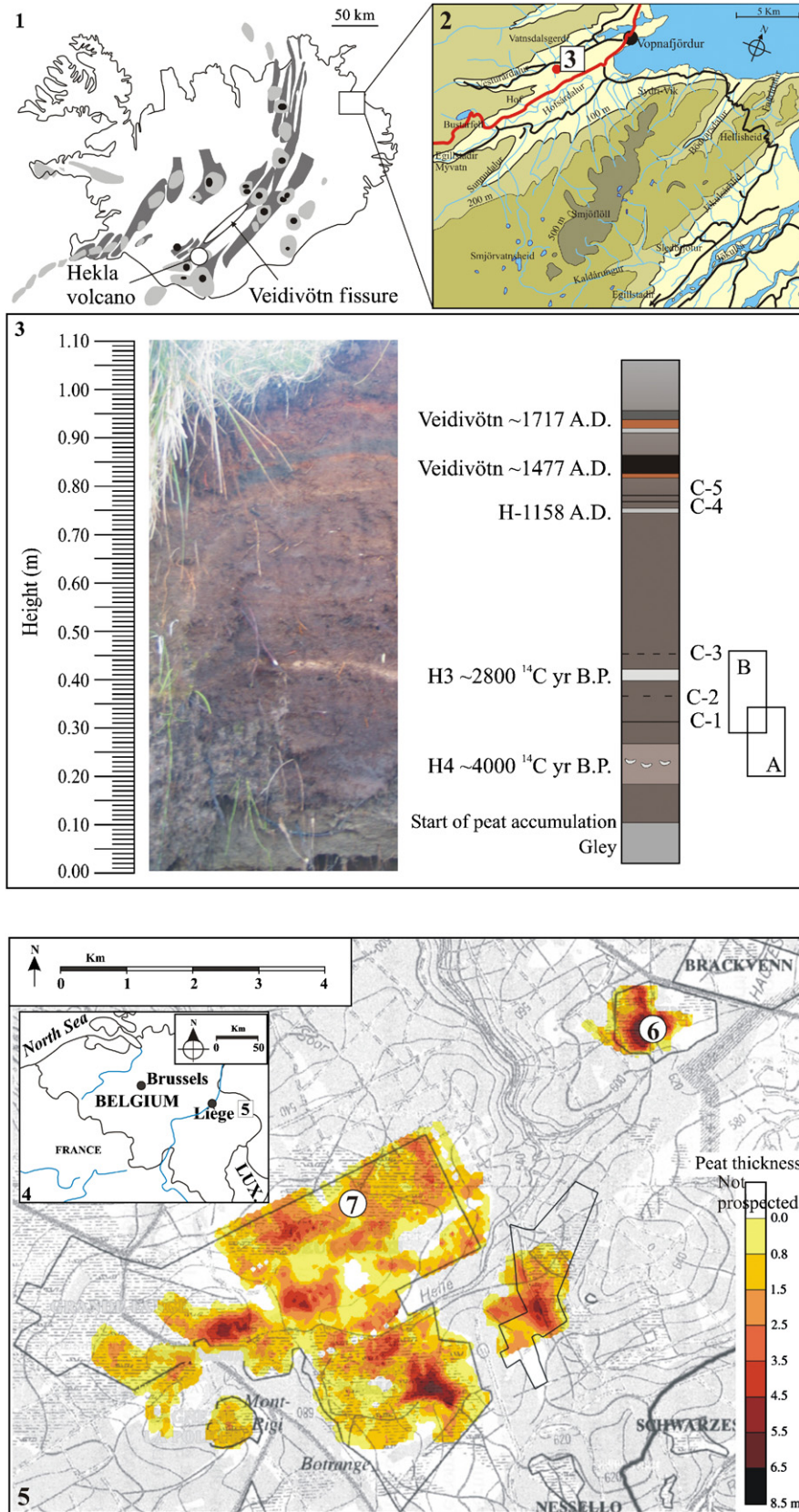


Fig. 2. Location maps (1, 2), photo and corresponding log (3) of a peat outcrop in the Vopnafjörður area (65°44' N–15°54' W). Five tephras were identified from field- and laboratory-based macroscopic observation (Hekla H4, H3 and H1158; and Veidivötn 1477 A.D. and 1717 A.D.). Five cryptotephras of unknown origin have been detected on impregnated thin sections (C1–C5). (A) and (B) refer to sections analysed using XRF logging (see Fig. 3). Location map (4, 5) showing the locations where the *Sphagnum*-dominated peat core was retrieved (6) and where the pumice deposit experiment (7) takes place. Peat thickness after Wastiaux and Schumacker (2003).

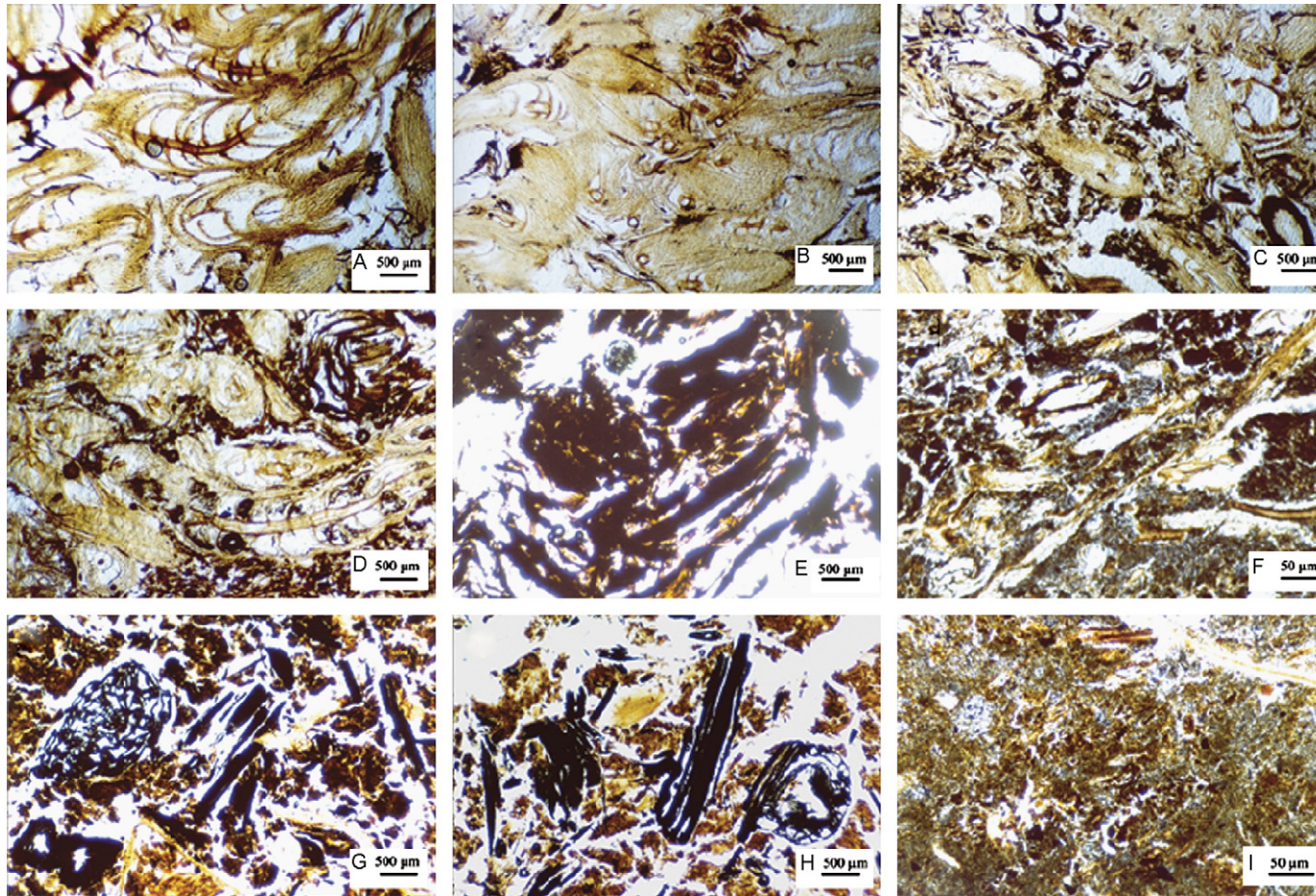


Fig. 3. Optical microscope pictures of organic structures (A–E) and charcoals (G and H) from a *Sphagnum*-dominated bog from southeast Belgium. Tephra (F and D) in peat from northeast Iceland. (A) Well-preserved *Sphagnum* stems and leaves at 30 cm depth. (B) Compacted *Sphagnum* tissues, 45 cm depth. (C) (50 cm depth) and (D) (80 cm depth) Progressive degradation of organic matter around the largest plant macrofossils and shift in peat composition, together with undefined mosses. (E) Highly decomposed peat at 640 cm depth. (F) Top of H-3 layer, strongly bioturbated by roots, with oxidation preferentially localised around roots. (I) H3 middle part of H-3 tephra showing strong oxidation.

(e.g. Moreno, 2000). Here, in situ observations of impregnated thin section can increase counting resolution allowing charcoal micro-layer detection. For example, Fig. 3G and H show charcoal layers in a Belgian peat bog. However, charcoal fragments found in thin sections do not allow a systematic identification of the species and should therefore be compared with handpicked fragments using traditional techniques such as scanning electron microscopy (SEM).

Micromorphological observation of peat can also be useful to determine to which level peat is humified, bioturbated, oxidised, or burned. Finally, inorganic layers such as dust, minerals or tephra deposits can be detected, counted, and their grain size can be estimated. However, such mineral objects are characterized more precisely by using a polarising microscope.

3.2. Polarising microscopy

The use of a polarising microscope allows characterization of inorganic components. Tephra layers can be studied for their mineralogical composition, texture and colour. Mineralogical identifications are possible if the thickness of the thin section is known. Bioturbated tephra can also be detected. Various types of coatings around tephra grains can be identified, such as short-range order clayey compounds (i.e. allophane), organic coatings or iron oxides.

As an example, a peat outcrop from Iceland containing tephra is presented in Fig. 2. Several tephra layers were identified in the field, including the H-4 tephra (~4000 ¹⁴C B.P., e.g. Larsen and Thorarinsson, 1977; Larsen et al., 1999), Hekla H-3 (~2800 ¹⁴C B.P., Larsen and Thorarinsson, 1977; Larsen et al., 1999), Hekla H-1158 AD (Larsen, pers. comm.), Veidivötn-1477 A.D., and V-1717 A.D. (e.g. Boyle, 1999). The top of H-3 layer is strongly bioturbated by roots (Fig. 3F). Moreover, although rhyolitic tephra seem to be homogenous on the field, Fig. 3I shows that some internal parts are strongly oxidised.

A careful inspection of the thin section allows the identification of five additional cryptotephra layers labelled C-1 to C-5, not detected during field and laboratory-based macroscopic investigations. The identification of these new distal tephra layers enhances the tephrostratigraphy of this exposure and their potential occurrence in other areas may provide a reinterpretation of the Holocene tephra succession of northeast Iceland. Cryptotephra C-1, C-4 and C-5 are represented by continuous layers of greyish to greenish scoriae, whereas C-2 and C-3 are discontinuous scoriae grain accumulations reworked by bioturbation. In Fig. 4A, cryptotephra C1 is shown. It is composed of scoriae up to 400 µm, opaque minerals, and some rare transparent minerals. The top of this tephra is strongly oxidised as shown by opaque minerals and some scoriae strongly coated by Fe oxides on the top right of Fig. 4A (arrow). Such oxidation of basaltic tephra could cause poor quality chemical analyses, even on single glass shards. Cryptote-

phra C3 consists of sparse scoriae grains (Fig. 4B) forming a discontinuous, sub-millimetre-thick layer, strongly affected by rootlets penetrating the surrounding peat.

In some cases, concentrations of mineral grains should be interpreted with caution. For example, a high concentration of transparent minerals (plagioclase) is shown in Fig. 4C. Although this might be interpreted as a cryptotephra, the round shape and generally fine grain size (<100 µm) suggests an aeolian origin. Indeed, Icelandic loess and andosols are generated inland from parent materials of volcanic origin (Arnalds, 2004). On the bottom of Fig. 4C, large (≥100 µm) Fe-oxide grains are also present (arrows). Though less abundant, these Fe-oxides were also seen coating fine glass shards in H-3 ash layer. Moreover, oxidation seems to be related to root penetration as suggested by the strong oxidation of H-3 around roots (Fig. 4D, arrows). This oxidation starts by bacterial attack. This feature could be missed after lab treatment of the glass shards, but can be observed in situ on impregnated thin sections. Fig. 4E shows a small transparent glass shard under bacterial attack, shown as filaments. These filaments cause the diffusion of elements from the glass to its edge, forming an alteration film around the glass shard. When more strongly attacked, glass shards are invisible. Together with bacterial filaments, these glass shards form strongly oxidised pellets, as shown on Fig. 4F. When these pellets aggregate together, a pelloid is formed and can rework fresh particles as shown on Fig. 4G.

3.3. Fluorescence microscopy

Fluorescence microscopy (UMR-PBDS, Lille, France) allows various coatings around tephra grains to be identified. In fluorescence microscopy, the light source is generally composed of an Hg arc with a discrete spectrum of emission or a deuterium lamp with a continuous spectrum. The light provides an exciter, which induces a new radiation from the sample, usually of a longer wave length than the excitation light. Assigning various filters to the light allows part of the lamp spectrum to be covered. Using a blue excitation filter (230 nm) is particularly efficient for the detection of organic matter and related alteration products. Indeed, Si-O bonds are partially broken by hydration, leading to partial glass dissolution producing a weathered layer commonly called palagonite. Crovisier et al. (2003) divided palagonite into two categories. The first category is characterized by an amorphous silica-rich gel resulting from simple glass hydration. This feature was also observed under experimental dissolution by, e.g., Berger et al. (1987). Daux et al. (1997) argued that this amorphous gel is composed of $\text{SiO}_2 + \text{Al}(\text{OH})_3 \pm \text{Fe}(\text{OH})_3 \pm \text{Ca}(\text{OH})_2 \pm \text{Mg}(\text{OH})_2$. The second category is a clayey mineral. For example, Silber et al. (1999) observed very fine halloysite-like allophane particles after glass dissolution at acidic pHs, and Techer et al. (2001) observed coatings on weathered glass. Both

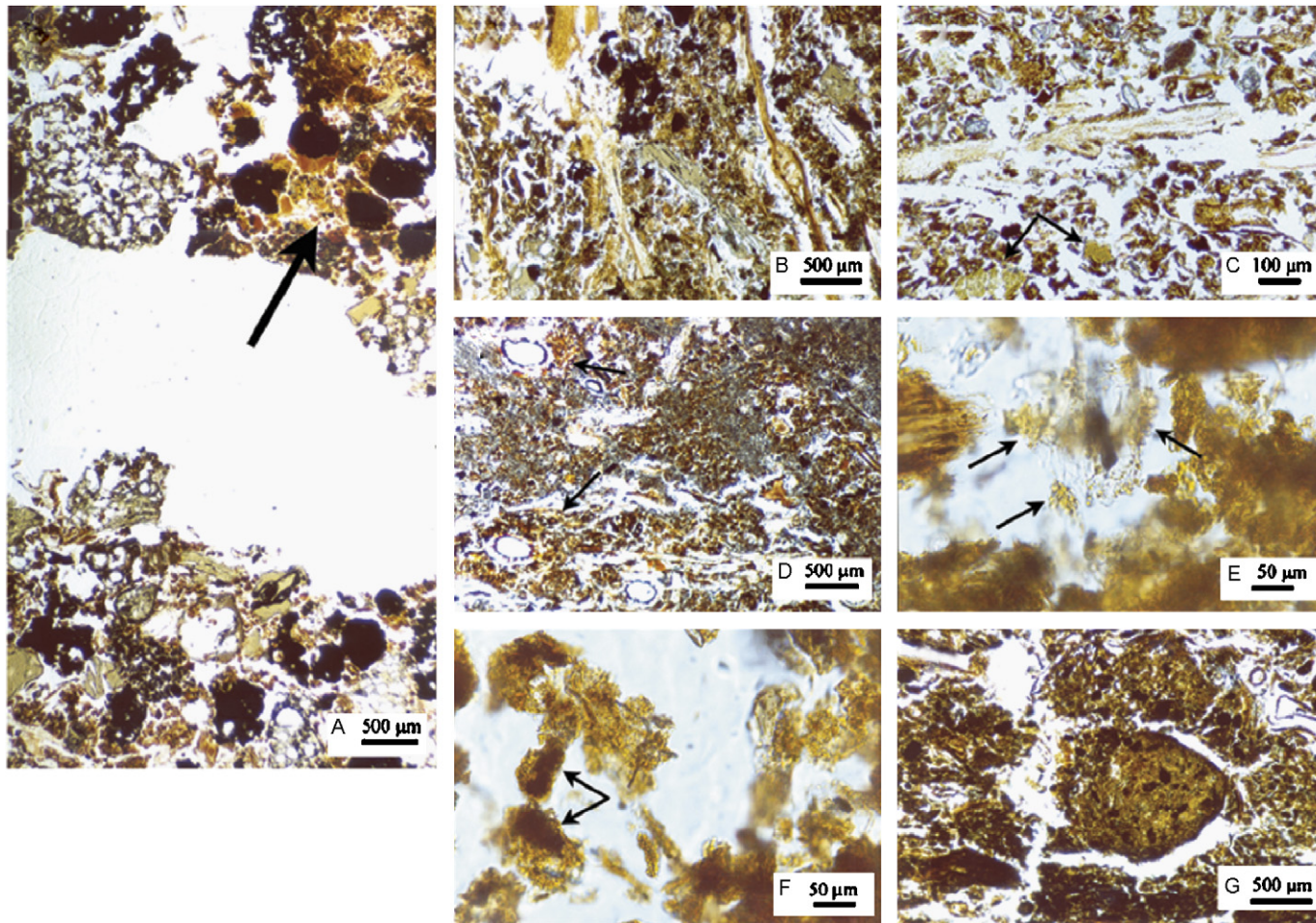


Fig. 4. Polarising microscope pictures of macro- and cryptotephra, and related alteration features. (A) Cryptotephra C1 with 1.5 mm crack artefact caused by shrinkage during freezing step of the sample. C1 is composed of scoriae, opaque minerals, rare transparent minerals. Opaque minerals scoriae are coated by Fe oxides at the top (arrows). (B) Discontinuous, sub-millimeter-thick Cryptotephra C3, consisting in sparse scoriae grains, strongly affected by rootlets penetrating the surrounding peat. (C) Round shape and fine grain size plagioclase from aeolian origin and large Fe-oxide grains (arrows). (D) Fe-oxides related to roots in H-3 tephra (arrows). (E) Transparent glass shard of H3 under filament bacterial attack (arrows). (F) Strongly oxidised pellets formed by aggregation of bacterial filaments and glass shards (G) Pelloidal aggregate reworking fresh particles.

studies came to the conclusion that this palagonitization leads to slowing down reaction kinetics. However, Pollard et al. (2003) emphasise the increasing relative instability of glass shards from acidic tephra to basaltic ones, and Hodder et al. (1991) reported how glass and ferromagnesian minerals in very acidic anoxic peat bogs were able to be partly or totally dissolve, leading sometimes to complete dissolution (e.g. biotite in relative short time periods). These different observations lead to the conclusion that a systematic microscopical control of core sediments, tephra, and related alteration products is useful when studying distal tephra in acidic environments.

The fluorescence properties of clay and colloidal materials are linked to the type of adsorbed cations. The order of effect of these cations is: $\text{Al}^{3+} > \text{Na}^+ > \text{K}^+ > \text{Mg}^{2+} > \text{Ca}^{2+} > \text{H}^+$ (Altemüller and Van Vliet-Lanoë, 1990). For example, van Vliet-Lanoë (1980) has shown that some polymers of aluminium hydroxides are responsible for a yellowish-green fluorescence in blue light. Iron compounds, in contrast, diminish the fluorescence effect towards complete extinction. With blue excitation, a more yellowish-brown colour is often present. Amorphous silica gel coatings on silicic minerals, such as on feldspars or glass shards, follow a pattern from light greenish to greenish yellow through the corrosion path. Other amorphous silica particles such as phytoliths or diatoms also display a greenish fluorescence in blue light. Using fluorescence microscopy on weathered tephra grains thus allows different kinds of alteration films to be distinguished.

Because it is composed of organic ligands and impurities, the resin will also display a fluorescent dark green colour. However, this fluorescence does not interfere with the observation.

Fig. 5 shows some typical alteration features of tephra in normal light (Fig. 5A–C, G and I) and blue light (Fig. 5D–F and H) light. For example, pelloidal aggregates (Fig. 5A and D arrowed) are strongly yellowish fluorescent, and less brownish in their centre, suggesting zoning in alteration between an Fe-rich centre and an Al-rich alteration rim. Alteration of scoriae results in greenish to yellowish alteration coatings (Fig. 5B and E) because the glass shards are increasingly weathered towards the edge of the grain. The darkness or yellowness of the colour depends on the proportion of Fe^{3+} and Al^{3+} in the alteration rim. Larger pelloidal aggregates (Fig. 5C and F) are strongly yellowish fluorescent since they are rich in organic matter. They are often reworking partially weathered glass shards in their early stage of aggregation (Fig. 5G and H).

3.4. SEM

Polished peat blocks can be coated (Au, Pt, or C) and placed in the pressurised chamber of a SEM. This allows observation of very small features such as allophane particles, bacterial tubes or tephra alteration scars. For

example, Fig. 6 shows some typical features observed on SEM backscattered electron images of impregnated peat sections. Bacterial attack seems critical in the tephra alteration process. Bacteria and algae are very common, as are the primary weathering media, developing tubing inside glass structures (Fig. 6A and B) and breaking down the glass shards (Fig. 6B). An experiment to examine the effect of alteration on glass in peat bogs showed that fresh pumice deposited on the surface of a Belgian peat bog (see Fig. 2 for location) over 2 years led to observable algae filament activity breaking glass walls (Fig. 6D). Several studies have provided insights into the effects of bacterial activities on glass dissolution. For example, Thorseth et al. (1995) found experimentally that the dissolution rate can increase by a factor of 10 after 6 months of glass alteration because of the formation of new bacterial communities. However, although their physical action could induce a rapid destruction of the glass walls, bacteria will also form and/or adsorb amorphous particles (from organic or mineral composition) at the grain surface, developing an alteration film that could decrease or stop the alteration of tephra. Such protective barrier films have been studied in the case of basaltic glass alteration and the use of basaltic glass as a radioactive stockpile (e.g. Techer et al., 2001). These different coatings that can cover mineral or glass particles were also observed, including bacterial tissues (Fig. 6C), Fe–Si–Al amorphous particles (Fig. 6E) or isolated allophane aggregates (Fig. 6F).

4. Geochemical applications

Impregnation of soft organic material opens the way to new possibilities for geochemical analyses. Although peat bogs are widely studied for their inorganic elemental (e.g. Kempter and Frenzel, 1999) and isotopic (e.g. Le Roux et al., 2005) content, this is usually achieved at a 1 cm-step at best. Moreover, excluding some studies of individual moss species (e.g. Martins et al., 2004), these analyses were performed on bulk samples. It could therefore be interesting to analyse the elemental content of specific plant fragments. With respect to studies on tephrostratigraphy and alteration processes, cryptotephra can be analysed for their geochemical content on the uncovered slide following detection by optical microscopy. Alteration products can be more easily selected for geochemical analyses. Isolating alteration products from a fresh core or from the surface of a tephra grain prior to single point analysis is challenging.

In the following paragraphs, we examine new insights into several techniques applied to impregnated peat blocks and thin sections. The major problem concerns the possible interaction of the resin itself with the beam of the analyser. Moreover, as the polymer for impregnation used is principally composed of C, H, and O, with traces of cobalt (catalyst), those elements cannot be measured. Finally, because the resin will have a single elemental signature, it is important to characterize it prior to analysing the sample to allow bias caused by the resin to be excluded.

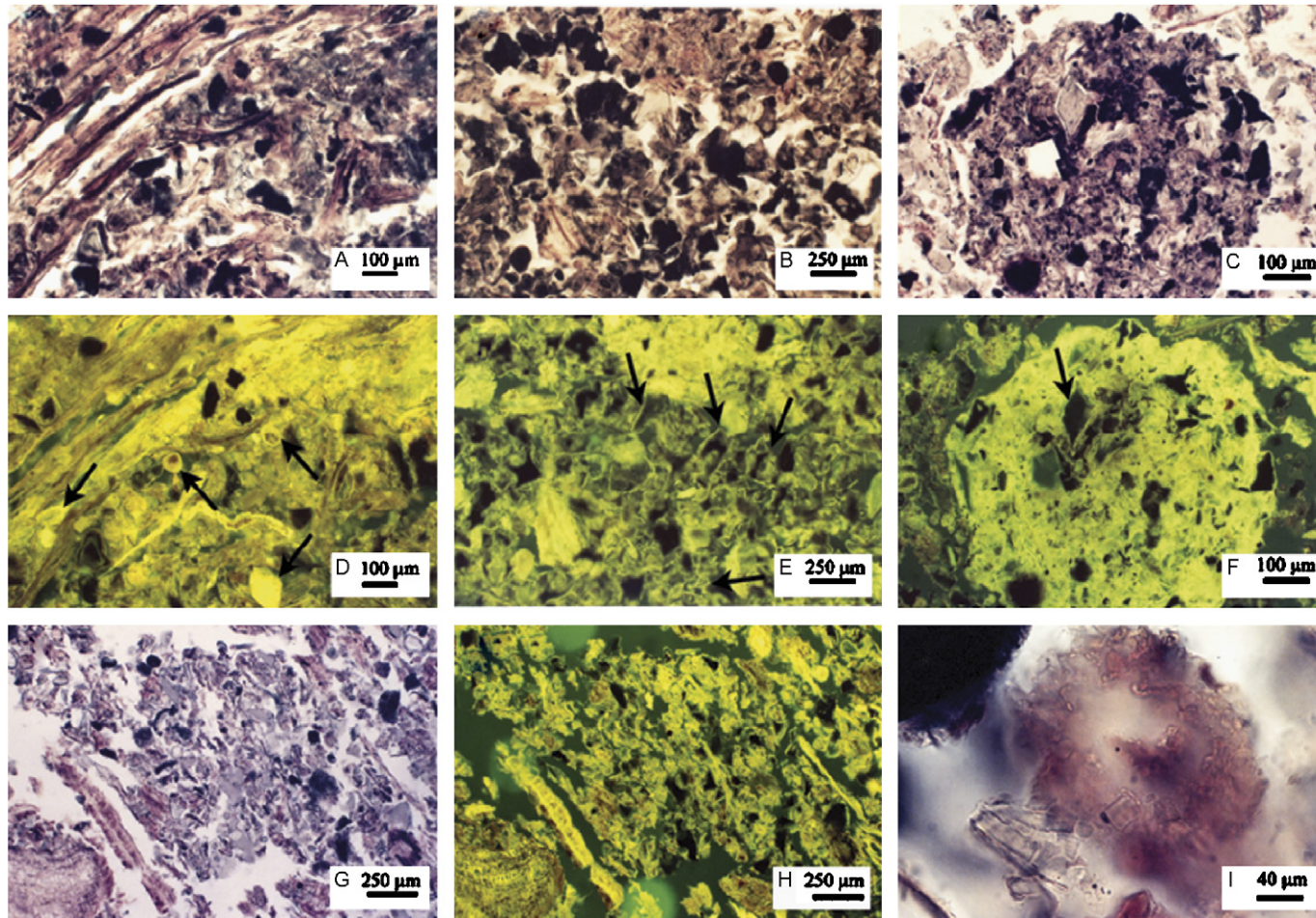


Fig. 5. Fluorescence microscope pictures of alteration features of tephras. The greenish overall colour of pictures is due to the UV-stop filter avoiding any retina damage during observation. (A) and (D) Pelloidal aggregate in normal and in blue light (yellowish grains arrowed). The less brownish colour suggest an increase in Fe content and decrease of Al content towards the centre of the grains. (B) and (E) Greenish to yellowish alteration coating around scoria grains (seen in normal and arrowed in blue light). The darkness or yellowness of the colour depends on the proportion of Fe^{3+} and Al^{3+} in the alteration rim. (C) (normal light) and (F) (blue light) Large pelloidal aggregate rich in organic matter (thus strongly yellowish in blue light), reworking glass shards. (G) (normal light) and (H) (blue light) Early pelloidal aggregation reworking scoriae which are coated with an alteration rim (yellowish edges in blue light). (I) Aggregation of bacterial filaments seen in normal light.

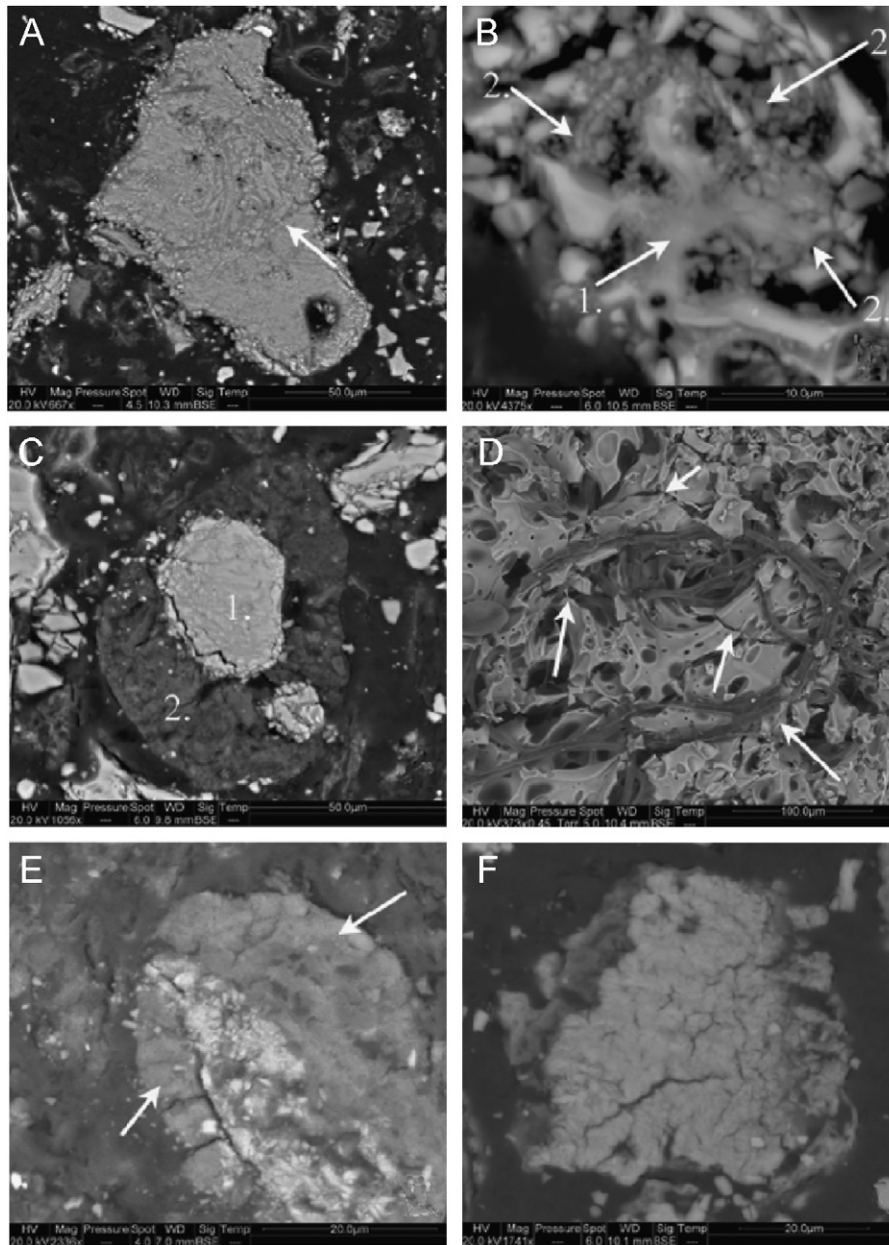


Fig. 6. Backscattered electron image of tephra alteration features observed by SEM on polished impregnated peat sections from Iceland. (A) and (B) Bacterial filaments (arrows) digging into a glass fragment. (C) Mineral grain (1) entirely covered by a complex bacterial web (2). (D) SEM backscattered electron image of a fresh pumice selected and prepared from Laacher See Tephra, Eifel (Germany) after 2 years of deposition on a peat surface of Belgium. The pumice is broken up by bacterial filaments (arrows). (E) Allophane coating (arrows) a mineral fragment. (F) Allophane aggregate presenting typical cracked structure.

4.1. XRF core-scanning

An early rapid XRF method has been used successfully (Lowe et al., 1981; Gehrels et al., 2006) on bulk peat samples from New Zealand to detect silicic tephra layers and Fe-rich tephra layers. However, though efficient and rapid, this technique only allowed a resolution step of 4 cm (as ~3.5 g of material is needed for classical XRF). It was also destructive as the samples were dried and powdered.

X-ray fluorescence (XRF) core scanning (Jansen et al., 1998; Richter et al., 2006) provides rapid, non-destructive

analyses on split sediment cores of a broad range of major, minor and trace elements (atomic mass range Al–U). This technique is commonly applied to marine and lacustrine sediment cores (e.g. Jansen et al., 1998; Haug et al., 2001). The surface of split cores has to be carefully flattened in order to reduce effects of surface roughness, thus improving the signal-to-noise ratio of XRF logging records. For peat cores, such surface smoothing is virtually impossible because peat is composed of plant macrofossils, together with fine material and roots. One advantage of the impregnation technique is that polished impregnated

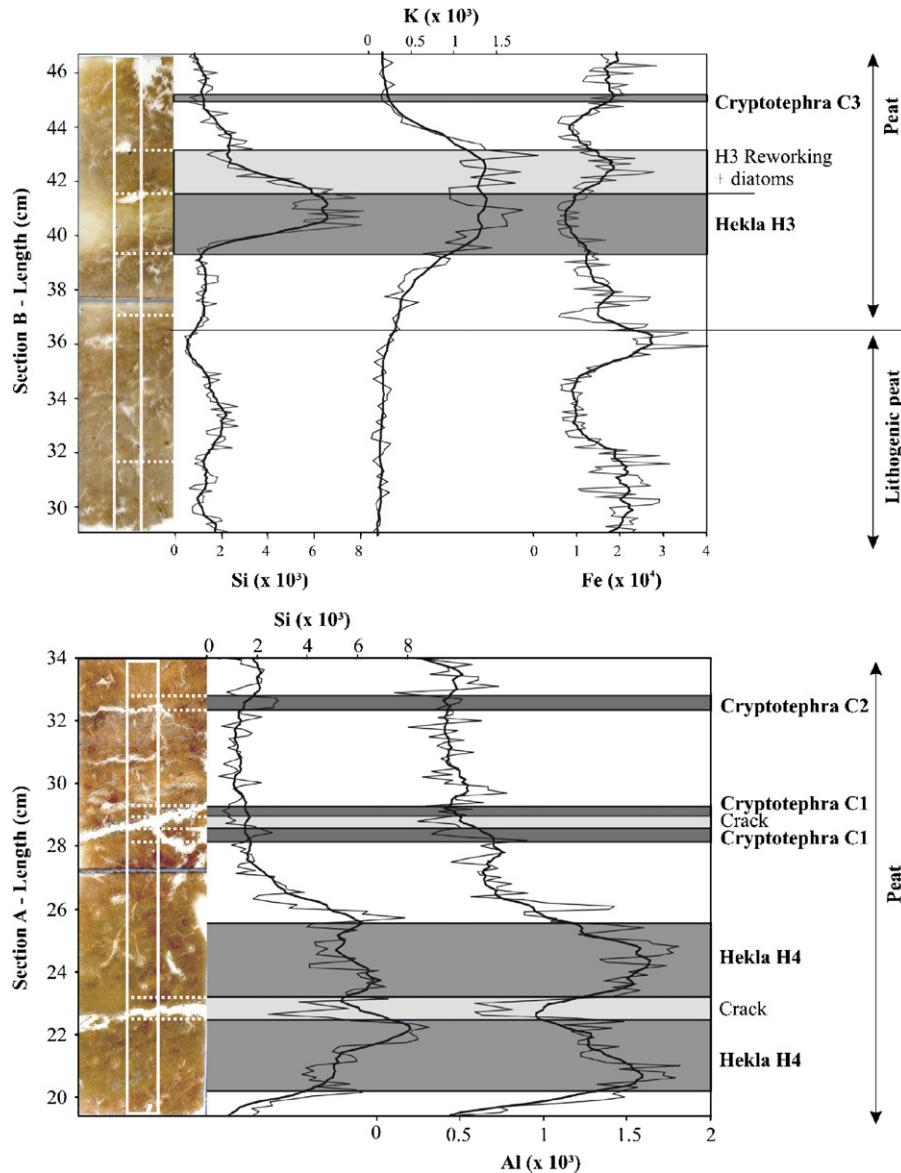


Fig. 7. One mm-step geochemical pattern (thin lines) and corresponding 1cm-mobile mean (bold lines) of two impregnated peat sections from Vopnafjörður outcrop (see Fig. 2). H4 and H3 tephras are present on these sections, together with C1–C3 cryptotephras.

blocks have a perfectly smooth surface. A spatial resolution of 1 mm can be achieved, potentially allowing for detection of fine structures such as cryptotephra particles, dust layers, and concentrations of clayey material. However, possible geochemical artefacts resulting from the chemical composition of the resin need to be critically assessed, and the presence of cracks may complicate detection of fine-scale sedimentary structures.

Since the resin contains a cobalt accelerator, resin-filled cracks may exhibit higher Co count rates and low counts for other elements. The resin was analysed for its chemical composition, and as all elements other than Co were below the detection limit, geochemical patterns for elements relevant for tephra studies will thus not be affected or biased. The XRF logging results are presented as number of XRF counts, tracing downcore geochemical variability

in the sedimentary column. Quantitative geochemical interpretation of bulk sediment data has not been attempted yet. It would require corrections for sediment porosity, which is high in peat deposits but likely to be variable on a small spatial scale, calibration based on standards with a similar organic-rich matrix, and validation by destructive quantitative analyses on selected depth intervals.

Fig. 7 shows the first results obtained by 1 mm logging with the Avaatech XRF Core Scanner (Royal NIOZ, Texel, Netherlands) on two impregnated sections from the Iceland outcrop (see Fig. 2). The two visible rhyolitic Hekla tephra layers H-3 and H-4, can be clearly identified based on XRF records of Si (Si_{H4} : 5000–9000 counts; Si_{H3} : 5000–8000 counts), Al (Al_{H4} : 1000–1600 counts) and K (K_{H3} : 500–1500 counts) values at least 2–3 times higher

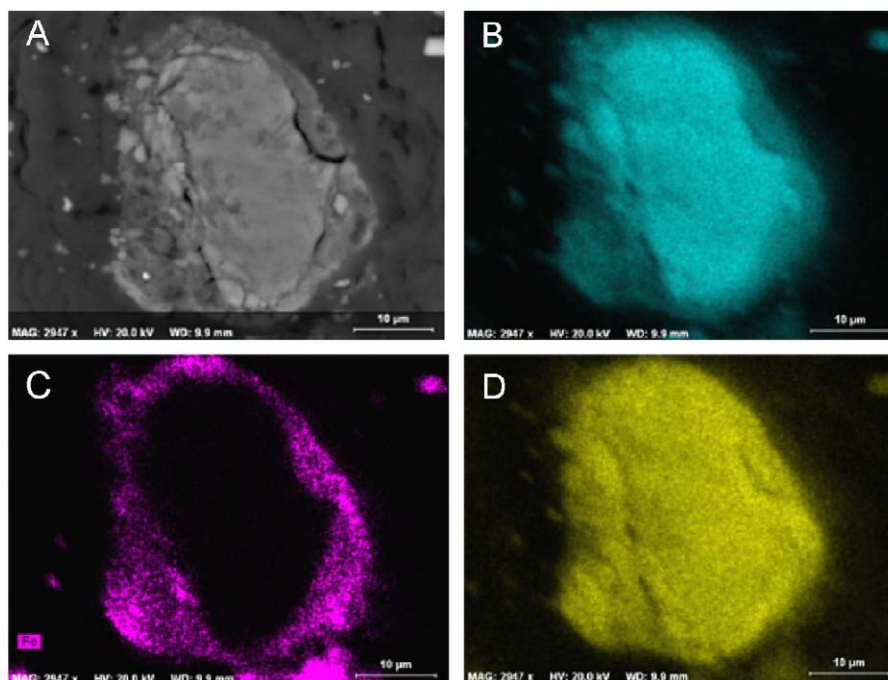


Fig. 8. Elemental mapping of a glass shard and its alteration rim given in relative concentration (i.e. the brighter on the picture, the richer in the given element). (A) Backscattered electron picture of the grain. (B) Elemental mapping of Si. (C) Elemental mapping of Fe. (D) Elemental mapping of Al.

than “background” peat levels. A slightly more lithogenic layer, not detected during field observations is also evident in Fe and Si profiles between 30 and 36 cm depth. Based on microscopic characterization, this layer consists of lithogenic peat, i.e. composed of organic material, variable amounts of amorphous Fe oxides, scattered basaltic scoriae and mineral fragments (probably washed and blown on the peat surface during erosion), bacterial filaments together with some dispersed diatoms. The relative variation explains the fluctuations in geochemical profiles. For example, Fe-enrichments around 36 cm are linked with an Fe-oxide-rich layer, while Fe-depletion around 34 cm is due to a decrease in Fe oxides together with an increase of the organic fraction relative to other components.

The three cryptotephra are not readily apparent in the XRF logging records. Parts of C1 and C2 show somewhat higher Si count rates, yet these values are only slightly elevated compared with rates for background peat deposits. In any case, a few dispersed volcanic grains will not necessarily affect the *bulk* geochemical composition of the corresponding depth interval. Particularly, at this location, basaltic cryptotephra layers may not be distinguishable from the background lithogenic fraction solely based on geochemical data. The background lithogenic component is presumably related to soil erosion in the vicinity of the peat bog, and these soils are themselves derived from alteration of basaltic parent material. The limited response depth of elements to incoming X-ray radiation (1 mm for Fe, but only ~ 0.05 mm for Al) also needs to be taken into account (Richter et al., 2006 and references therein), because the XRF scanning method will

not ‘detect’ grains further below the surface of the impregnated core section. In sum, although substantial tephra layers leave a clear signature in XRF logging records, cryptotephra cannot be readily detected. Interpretation of minor variability in elemental geochemical records needs to be accompanied by microscopic observations of corresponding thin sections.

Future developments in XRF logging have the potential for higher spatial resolution, down to a step size and irradiated surface area of 0.1 mm in downcore direction. This level of resolution may help to constrain the identification of cryptotephra layers through detection of individual tephra grains. On the other hand, a smaller irradiated surface area necessarily implies a decrease in sensitivity of XRF logging, particularly for light elements such as Si and Al. Moreover, a poorer overall signal-to-noise ratio is also to be expected: some variability at sub-mm spatial resolution will probably reflect small-scale variability in porosity, which results in higher elemental count rates for lithogenic peat and low values for intervening pore spaces.

4.2. SEM-EDS

If a SEM is equipped with an energy dispersive system (SEM-EDS, UMR-PBDS, Lille, France), polished impregnated samples can be analysed for geochemical content, principally major elements, without any re-sampling. Elemental surface mapping is also possible. An example of a glass grain and its alteration rim composed of an Fe–Al–Si coating, analysed in an impregnated sample from North Iceland, is given in Fig. 8. The backscattered

electron image (A) is followed by the relative concentration of Si (B), Fe (C) and Al. (D). Silicon is very abundant in the centre of the mineral. However, it is also present on the rim, together with a strong enrichment in Fe. Al is also a main component, but shows no zoning between the centre and the alteration rim.

5. Other techniques

Electron microprobe analysis on non-covered thin sections or on polished impregnated samples could be achieved and point characterisation could be acquired (Sinkankas, 1968). For example, this technique could be useful to determine the precise composition of an alteration rim around glass shards, or to investigate compositional variation around rootlets.

Physical properties could also be measured in the same way as on a fresh core. However, because their variations reflect changes in sediment composition and grain-size, they have to be accompanied by microscopic observations. Although not tested on impregnated peat containing tephros, magnetic susceptibility gave promising results on impregnated lacustrine sediments (Boës et al., 2005) and on peat containing tephros (Develle et al., 2006).

Finally, although not achieved yet in our study, X-ray radiography should be possible on impregnated blocks as it was successfully achieved on fresh and dried cores by, e.g., Lowe et al. (1981), because the resin is mainly composed of light elements (C, H, O) which will be transparent to the beam.

6. Conclusions

The impregnation of peat deposits can reveal information concerning their state of preservation, vegetation type, and the presence of charcoal or mineral particles. More specifically, the impregnation of tephra-containing peat sections and their subsequent study in thin section using various techniques allows a broad range of observations useful not only for the field of tephrostratigraphy but also for studies of tephra alteration mechanisms and by-products, for discriminating between reworked or in situ tephra and for detecting of cryptotephros. It has potential for a wide range of chemical investigations leading to a better understanding of the chemical signature of tephros and their alteration products.

Acknowledgements

Frédéric Boulvain and Jean-Paul Cullus were of great help in the thin section preparation. We would also like to warmly thank Rineke Gieles (NIOZ, Texel, The Netherlands) and Philippe Recourt (UMR-PBDS, Lille, France) for their assistance with XRF logging and SEM-EDS analysis, respectively. We are grateful to Maria Gehrels, David Lowe, Duane Froese and one anonymous reviewer for their enthusiastic comments and English smoothing.

The impregnation laboratory at URAP has been developed and optimised thanks to University fund Nr R.CERA.0438. This work is also supported by the French program IPROCI, funded by the Institut Paul Emile Victor (Iceland field mission and SEM-EDS analysis). François De Vleeschouwer is supported by a FRIA fellowship.

References

- Altemüller, H.J., Van Vliet-Lanoë, B., 1990. Soil thin section fluorescence microscopy. In: Douglas, J.A. (Ed.), *Soil Micromorphology, a Basic and Applied Science. Developments in Soil Science*, vol. 19, pp. 565–576.
- Arnalds, O., 2004. Volcanic soils of Iceland. *Catena* 56, 3–20.
- Berger, G., Schott, J., Loubet, M., 1987. Fundamental processes controlling the first stage of alteration of a basalt glass by seawater: an experimental study between 200 and 320 °C. *Earth and Planetary Science Letters* 84, 431–445.
- Boës, X., Fagel, N., 2005. Impregnation method for detecting annual laminations in sediment cores: an overview. *Sedimentary Geology* 179, 185–194.
- Boës, X., Piotrowska, N., Fagel, N., 2005. High resolution diatom/clay record in Lake Baikal from grey-scale, and magnetic susceptibility over Termination I. *Global and Planetary Change* 46, 299–313.
- Boyle, J.E., 1999. Variability of tephra in lake and catchment sediments, Svinavatn, Iceland. *Global and Planetary Change* 21, 129–149.
- Camuti, K.S., McGuire, P.T., 1999. Preparation of polished thin sections from poorly consolidated regolith and sediment materials. *Sedimentary Geology* 128, 171–178.
- Caseldine, C., Baker, A., Barnes, W., 1999. A rapid, non-destructive scanning method for detecting distal tephra layers in peats. *The Holocene* 9, 635–638.
- Crovisier, J.-L., Advocat, T., Dussossoy, J.L., 2003. Nature and role of natural alteration gels formed on the surface of ancient volcanic glasses. Natural analogues of waste containment glasses. *Journal of Nuclear Materials* 321, 91–109.
- Daux, V., Guy, C., Advocat, T., Crovisier, J.-L., Stille, P., 1997. Kinetic aspects of basaltic glass dissolution at 90 °C: role of aqueous silicon and aluminium. *Chemical Geology* 142, 109–126.
- Develle, A.-L., Walter-Simonnet, A.-V., Bossuet, G., Rossy, M., Begeot, C., Ruffaldi, P., Adatte, T., 2006. Retombées de cendre volcaniques durant le Tariglacière et l'Holocène—Quelques exemples d'enregistrement du Jura aux Vosges. In: *Le Quaternaire, limites et spécificités, Proceedings Colloque Q5, Paris, 1–3 février 2006 (in French)*.
- Dugmore, A.J., Newton, A.J., 1992. Thin tephra layers in peat revealed by X-radiography. *Journal of Archaeological Science* 19, 163–170.
- Fisher, R.V., 1964. Maximum size, median diameter and sorting of tephra. *Journal of Geophysical Research* 69, 341–355.
- Francus, P., 1998. An image-analysis technique to measure grain-size variation in thin-sections of soft clastic sediments. *Sedimentary Geology* 121, 289–298.
- Gehrels, M.J., Lowe, D.J., Hazell, Z.J., Newnham, R.M., 2006. A continuous 5300-year Holocene cryptotephrostratigraphic record from northern New Zealand and implications for tephrochronology and volcanic hazard assessment. *The Holocene* 16, 173–187.
- Gehrels, M., Newnham, R.M., Lowe D.J., Wynne, S., Caseldine, C., this volume. Potential methods for developing a rapid assay of cryptotephra in peat cores.
- Haug, G.H., Hughen, K.A., Sigman, D.M., Peterson, L.C., Röhl, U., 2001. Southward migration of the intertropical convergence zone through the Holocene. *Science* 293, 1304–1308.
- Hodder, A.P.W., De Lange, P.J., Lowe, D.J., 1991. Dissolution and depletion of ferromagnesian minerals from Holocene tephra layers in an acid bog, New Zealand, and implications for tephra correlation. *Journal of Quaternary Science* 6, 195–208.

- Jansen, J.H.F., Van der Gaast, S.J., Koster, B., Vaars, A.J., 1998. CORTEX, a shipboard XRF-scanner for element analyses in split sediment cores. *Marine Geology* 151, 143–153.
- Jowsey, P.C., 1965. An improved peat sampler. *New Phytologist* 65, 245–248.
- Kempton, H., Frenzel, B., 1999. The local nature of anthropogenic emission sources on the elemental content of nearby ombrotrophic peat bogs, Vulkaneifel, Germany. *The Science of the Total Environment* 241, 117–128.
- Larsen, G., Thorarinsson, S., 1977. H₄ and other acid Hekla tephra layers. *Jökull* 27, 27–46.
- Larsen, G., Dugmore, A., Newton, A., 1999. Geochemistry of historical-age silicic tephra in Iceland. *The Holocene* 9, 463–471.
- Le Roux, G., Aubert, D., Stille, P., Krachler, M., Kober, B., Cheburkin, A., Bonani, G., Shoty, W., 2005. Recent atmospheric Pb deposition at a rural site in southern Germany assessed using a peat core and snowpack, and comparison with other archives. *Atmospheric Environment* 39, 6790–6801.
- Lotter, A.F., Lemcke, G., 1999. Methods for preparing and counting biochemical varves. *Boreas* 28, 243–252.
- Lowe, D.J., Hogg, A.G., Hendy, C.H., 1981. Detection of thin tephra deposits in peat and organic lake sediments by rapid X-radiography and X-ray fluorescence techniques. In: Howorth, R., Froggatt, P., Vucetich, C.G., Collen, J.D. (Eds.), *Proceedings of Tephra Workshop, 30th June–1st July 1980*, Publication of the Geology Department no. 20, Victoria University of Wellington, New Zealand.
- Mackenzie, A.F., Dawson, J.E., 1961. The preparation and study of thin sections of wet organic soil materials. *Journal of Soil Science* 12, 142–144.
- Martins, R.J.E., Pardo, R., Boaventura, R.A.R., 2004. Cadmium II and zinc II adsorption by the aquatic moss *Fontinalis antipyretica*: effect of temperature, pH and water hardness. *Water Research* 38, 693–699.
- Moreno, P.M., 2000. Climate, fire, and vegetation between about 13,000 and 9200 ¹⁴C.B.P. in the Chilean Lake District. *Quaternary Research* 54, 81–89.
- Naranjo, J.A., Stern, C.R., 1998. Holocene explosive activity of Hudson Volcano, southern Andes. *Bulletin of Volcanology* 59, 291–306.
- Newnham, R.M., Lowe, D.J., McGlone, M.S., Wilmshurst, J.M., Higham, T.F.G., 1998. The Kaharoa tephra as a critical datum for earliest human impact in Northern New Zealand. *Journal of Archaeological Science* 25, 533–544.
- Okuno, M., Nakamura, T., Kamata, H., Kobayashi, T., 2003. Radiocarbon dating of paleosols intercalated with tephra layers in Japan. In: Juvigné, E., Raynal, J.-P. (Eds.), *Tephra, Chronology, Archaeology, Dossiers de l'Archéo-Logis* 1, pp. 67–72.
- Pike, J., Kemp, A.E.S., 1996. Preparation and analysis techniques for studies of laminated sediments. In: Kemp, A.E.S. (Ed.), *Palaeoclimatology and Palaeoceanography from Laminated Sediments*. Geological Society of America Special Publication, vol. 116, pp. 37–48.
- Pollard, A.M., Blockley, S.P.E., Ward, K.R., 2003. Chemical alteration of tephra in the depositional environment: theoretical stability modelling. *Journal of Quaternary Science* 18, 79–93.
- Pusch, R., 1999. Experience from preparation and investigation of clay microstructure. *Engineering Geology* 54, 187–194.
- Richter, T.O., van der Gaast, S., Koster, B., Vaars, A., Gieles, R., de Stigter, H.C., de Haas, H., van Weering, T.C.E., 2006. The Avaatech XRF core scanner: technical description and applications to NE Atlantic sediments. In: Rothwell, G. (Ed.), *New Techniques in Sediment Core Analysis*. Geological Society London Special Publications, vol. 267, pp. 39–50.
- Sadler, J.P., Grattan, J.P., 1999. Volcanoes as agents of past environmental change. *Global and Planetary Change* 21, 181–196.
- Silber, A., Bar-Yosef, B., Chen, Y., 1999. pH-dependant kinetics of tuff dissolution. *Geoderma* 93, 125–140.
- Sinkankas, J., 1968. High pressure epoxy impregnation of porous materials for thin-section and microprobe analysis. *American Mineralogist* 53, 339–342.
- Takeda, H., 1988. A rapid method for preparing thin sections of soil organic layers. *Geoderma* 42, 159–164.
- Techer, I., Advocat, T., Lancelot, J., Liotard, J.-M., 2001. Dissolution kinetics of basaltic glasses: control by solution chemistry and protective effect of the alteration film. *Chemical Geology* 176, 235–263.
- Thorseth, I.H., Furnes, H., Tumyr, O., 1995. Textural and chemical effects of bacterial activity on basaltic glass: an experimental approach. *Chemical Geology* 119, 139–160.
- Tippkötter, R., Ritz, K., 1996. Evaluation of polyester, epoxy and acrylic resins for suitability in preparation of soil thin sections for in situ biological studies. *Geoderma* 69, 31–57.
- van den Bogaard, C., Schmincke, H.-U., 2002. Linking the North Atlantic to Central Europe: a high resolution Holocene tephrochronological record from northern Germany. *Journal of Quaternary Science* 17, 3–20.
- Van Vliet-Lanoë, B., 1980. Approche des conditions physico-chimiques favorisant l'autofluorescence des minéraux argileux. *Pédologie* 3, 369–390 (in French).
- Wastiaux, C., Schumacker, R., 2003. Topographie de surface et de subsurface des zones tourbeuses des réserves naturelles domaniales des Hautes-Fagnes. Convention C60 entre le Ministère de la Région Wallonne, Direction générale des Ressources naturelles et de l'Environnement, et l'Université de Liège. Unpublished report, 52p. + annexes (in French).
- Wulf, S., Kraml, M., Brauer, A., Keller, J., Negendank, J.F.W., 2004. Tephrochronology of the 100 ka lacustrine sediment record of Lago Grande di Monticchio southern Italy. *Quaternary International* 122, 7–30.